NASA Technical Paper 1015

A Study of the Sonic-Boom Characteristics of a Blunt Body at a Mach Number of 4.14

Harry W. Carlson and Robert J. Mack

SEPTEMBER 1977

NASA

NASA Technical Paper 1015

A Study of the Sonic-Boom Characteristics of a Blunt Body at a Mach Number of 4.14

Harry W. Carlson and Robert J. Mack

Langley Research Center
Hampton, Virginia

National Aeronautics
and Space Administration

**Scientific and Technical
Information Office**

1977

SUMMARY

An experimental and theoretical study of sonic-boom generation of a blunt body at a high supersonic Mach number has shown that for accurate measurement of sonic-boom flow fields with conventional static-pressure probes, strong pressure fields with large flow angularities should be avoided. Small models, for which larger nondimensionalized distances and thus weaker pressure fields can be obtained, are preferable to large models even with the sacrifice in construction accuracy and the demands placed on measurement systems. When the purpose of sonic-boom testing is the provision of data for use in existing geometric acoustic extrapolation methods, the limitations on overpressure are even more demanding because signature impulse is found to follow acoustical disturbance laws only for very weak flow fields. The most significant finding, however, is that the applicability of far-field sonic-boom theory previously demonstrated for more slender shapes may now be extended to bodies with ratios of diameter to length as great as two and to Mach numbers at least as high as 4.14. This last conclusion is particularly important in view of the limitations to the use of existing methods for extrapolation of close-in experimental data.

INTRODUCTION

A large number of wind-tunnel experimental programs (refs. 1 to 12) have been conducted to explore the nature of sonic-boom phenomena and to define the applicability of theoretical prediction methods. Generally, these studies demonstrated a rather remarkable ability of simplified theoretical methods (based primarily on refs. 13 to 16 and described in ref. 17) to provide accurate estimates of sonic-boom characteristics for a wide variety of bodies, wings, wing-body combinations, and complete supersonic aircraft configurations.

Little effort, however, has been devoted to an exploration of the applicability of the theory to very blunt body shapes at high supersonic speeds - shapes representative of entry vehicles and of exhaust gas plumes that develop behind ascending spacecraft and dominate the sonic-boom generation. Wind-tunnel tests of the Apollo command module and of the Saturn V-Apollo launch vehicle with a simulated exhaust plume (refs. 18 and 19) have provided data for extrapolations which correlated well with flight-test results (refs. 20 and 21). These wind-tunnel measurements, however, were made only in the extreme near field, and thus do not provide information on flow-field development over a range of distances sufficient for the testing of theories based on asymptotic approximations.

Because of small disturbance approximations made in its development, the theory is commonly believed to be invalid at hypersonic speeds and particularly so for blunt shapes. Nevertheless, in view of the past successes of the theory, it is believed prudent to explore carefully its limitations rather than to accept a priori its inapplicability under certain conditions.

The experiment described in this report provides data on the flow field generated by a blunt body, a paraboloid of revolution with a ratio of diameter to length of two, at a Mach number of 4.14. To provide sufficient data on the evolution of the flow field for comparison with far-field theoretical estimates, measurements of static pressures generated by models of two different sizes were made at distances from 2 to 32 body lengths. The extreme close-in distances were included to provide more information on signature development, and to help assess problems encountered in measurement of static pressures in strong shock fields. The models of different sizes aided in a study of the compromise between large models for accurate geometric definition and small models for generation of weak flow fields meeting the requirements of acoustical extrapolation methods.

SYMBOLS

A	cross-sectional area normal to body axis
D	body maximum diameter, base diameter
$F(\tau)$	area distribution function, $\frac{1}{2\pi}\int_0^{\tau}\frac{A''}{\sqrt{\tau - x}}\,dx$
h	perpendicular distance from model center line to measuring probe
K_r	reflection factor
l	model length
M	Mach number
p	reference pressure, free stream static
Δp	incremental pressure due to model flow field
Δp_A	adjusted incremental pressure at bow shock of measured pressure signature (see fig. 6(b))
Δp_b	incremental pressure at bow shock of theoretical pressure signature
r	body radius
x	distance measured along body longitudinal axis from body nose
Δx	longitudinal distance from point on pressure signature to point where pressure signature curve crosses zero-pressure reference axis
Δx_A	adjusted value of length of positive portion of measured pressure signature (see fig. 6(c))

Δx_b length of positive portion of theoretical pressure signature

β $= \sqrt{M^2 - 1}$

γ ratio of specific heats (1.4 for air)

θ angle between radial line through probe orifice and line between probe and model center lines (see fig. 3)

τ dummy variable of integration measured in same direction and using same units as x

τ_o value of τ giving largest positive value of integral $\int_0^{\tau} F(\tau)\, d\tau$

A prime is used to indicate a first derivative and a double prime is used to indicate a second derivative with respect to distance along the model axis.

MODELS, APPARATUS, AND TESTS

To obtain data for a wide range of distances from the model (expressed in terms of the model length), it was necessary to construct two models. These models illustrated in figure 1 had identical forebody shapes but differed in scale by a factor of 4. This made it possible to measure pressure signatures for the large model at nondimensionalized distances of 2, 4, and 8, and for the small model at nondimensionalized distances of 8, 16, and 32; these distances are well within the limited space of the wind-tunnel test section. The model forebodies are paraboloids defined by the equations shown in the figure. The sting supports for the models were designed to avoid the generation of a pressure disturbance ahead of the expansion from the forebody maximum diameter.

A sketch of the wind-tunnel test apparatus is also shown in figure 1. The model actuator, mounted on the tunnel sidewall, provided remotely controlled longitudinal motion for the model. Pressure probes, mounted on the permanent tunnel sting support system were capable of remotely controlled lateral and longitudinal movement. The tunnel sting support motion was used to place the model and the pressure sensing apparatus in the proper relative position and the model actuator was used to move the model from one position to another as the measurements were taken. The pressure-sensing apparatus was constructed so that the pressure signature of the model (all the signature ahead of the expansion from the forebody maximum diameter) could be registered by the sensing probe before the bow shock impinged on the orifices of the reference probe.

The probes were very slender cones (2^o cone half-angle), each having top and bottom orifices with a diameter of 0.089 cm. Note that a line connecting the pair of orifices is perpendicular to the horizontal plane containing the model and the probe. The selection of a pair of orifices rather than the previously used set of four with circumferential spacing of 90^o is discussed later. Other considerations to be taken into account in providing accurate wind-tunnel measurements of sonic-boom characteristics are given in references 22 and 23.

TEST CONDITIONS

The investigation was conducted in the Langley Unitary Plan wind tunnel at a Mach number of 4.14 with a stagnation pressure level of 0.20 MN/m^2 (29.55 psia) and a stagnation tempereature of 80° C (176° F).

THEORETICAL CONSIDERATIONS

The character of spacecraft configurations and their operational environment permit the use of far-field theory for sonic-boom predictions. The bluntness insures a rapid coalescense of shocks to produce a simple wave form early in the propagation and the high altitudes provide a sufficient time for the formation of classical far-field "N-wave" pressure signature.

The existing near-field theoretical prediction methods are, in fact, inappropriate for this application. The near-field numerical prediction methods (refs. 24 and 25) have been shown to provide detailed signatures which correlate well with measured signatures for supersonic cruise airplanes. However, the so-called near-field theories are based on a supposition that the generating bodies are long and slender and the disturbances weak; conditions which obviously are not met in the present investigation. It might be noted that the near-field theory gives signatures which in all cases are longer than those given by far-field theory for the same conditions; whereas, as will be seen, blunt shapes actually produce signatures very much shorter than those given by the far-field theory.

Another approach for the development of near-field (and far-field) prediction methods which may be applicable to blunt configurations is being pursued by L. Ting (ref. 26). This procedure which is based on the method of characteristics does not have the inherent limitations of the linearized theory methods on which present theories are based.

The far-field theory to be employed in this study is described in references 13 and 15. Discussions of the theory, development of numerical methods for its implementation, and numerous correlations with experimental data are given in reference 27.

In the following equations obtained from reference 15, the bow shock overpressure directly under the flight path of an aircraft in level supersonic flight is related to the geometry of the aircraft and the flight conditions:

$$\Delta p_b = p \frac{K_r \gamma (2\beta)^{1/4}}{(h)^{3/4}\sqrt{\gamma + 1}} \sqrt{\int_0^{\tau_o} F(\tau)\, d\tau} \qquad (1)$$

The length of the positive portion of the "N wave" pressure signature is given by

$$\Delta x_b = h^{1/4} \frac{(\gamma + 1)(2)^{1/4} M^2}{\beta^{3/4} \sqrt{\gamma + 1}} \sqrt{\int_0^{\tau_o} F(\tau)\, d\tau} \tag{2}$$

Thus the impulse or the area under the positive portion of the signature is

$$\int \Delta p\, dx = \frac{p}{\sqrt{h}} \frac{K_r \gamma M^2}{\sqrt{2\beta}} \int_0^{\tau_o} F(\tau)\, d\tau \tag{3}$$

For a body with no lift, the function $F(\tau)$ in equations (1), (2), and (3) depends only on the longitudinal distribution of cross-sectional area and is defined as

$$F(\tau) = \frac{1}{2\pi} \int_0^{\tau} \frac{A''(x)}{\sqrt{\tau - x}}\, dx$$

For previous studies in which the bodies were slender and the disturbances propagated along lines not too far different from Mach lines, area distributions as defined by supersonic area rule concepts were employed. In this instance, where the blunt shape forces the formation of a normal shock ahead of the nose, normal area distributions are believed to be more appropriate.

For the body shape chosen for this experiment, the theoretical sonic-boom characteristics may be determined by a completely analytic process. The area development is simply $A = \pi x l$. With proper care in handling a singularity in the second derivative of the area development at the nose, in a manner similar to that used in reference 28, the sonic-boom signature quantities become

$$\Delta p_b = p \frac{K_r \gamma (2\beta)^{1/4}}{\sqrt{\gamma + 1}} \frac{D}{2(h)^{3/4}(l)^{1/4}}$$

$$\Delta x_b = \frac{(\gamma + 1)(2)^{1/4} M^2}{\beta^{3/4} \sqrt{\gamma + 1}} \frac{(h)^{1/4} D}{2(l)^{1/4}}$$

$$\int \Delta p\, dx = p \frac{K_r M^2}{\sqrt{2\beta}} \frac{D^2}{4\sqrt{h}\sqrt{l}}$$

The signature characteristics may also be expressed in convenient parametric forms which, with γ set equal to 1.4, are

$$\frac{\Delta p_b}{p}\left(\frac{h}{l}\right)^{3/4} = K_r \beta^{1/4}(0.537)\frac{D}{l}$$

$$\frac{\Delta x_b}{l}\left(\frac{h}{l}\right)^{-1/4} = \frac{M^2}{\beta^{3/4}}(0.921)\frac{D}{l}$$

$$\int \frac{\Delta p}{p}\,\frac{dx}{l}\sqrt{\frac{h}{l}} = K_r\,\frac{M^2}{\sqrt{\beta}}(0.247)\left(\frac{D}{l}\right)^2$$

For the conditions of this test, the parameters become

$$\frac{\Delta p_b}{p}\left(\frac{h}{l}\right)^{3/4} = 1.52$$

$$\frac{\Delta x_b}{l}\left(\frac{h}{l}\right)^{-1/4} = 11.12$$

$$\int \frac{\Delta p}{p}\,\frac{dx}{l}\sqrt{\frac{h}{l}} = 8.44$$

Through use of these parameters, theoretical signatures for a given body at a given Mach number may be represented by a simple N-wave. Variations with distance are taken into account in the parameters. The far-field parametric form of signature presentation is particularly useful in analysis of experimental data. It may be used, as will be shown later, to assess the degree to which far-field conditions are approached and to evaluate the applicability of the theory.

RESULTS AND DISCUSSION

Basic data for the measured signatures at various distances are shown in figure 2. The ratio of the incremental pressures to the free-stream static value is plotted as a function of nondimensionalized distance from the zero incremental pressure point.

The cause of the double peaked behavior of the signatures in the vicinity of the bow shock, which is particularly noticeable for the close-in positions, is unknown. It may be the result of a shock—boundary-layer interaction. At larger distances where the shock strength is much reduced and the pressure peaks less sharply defined, the doubled peak behavior tends to disappear.

It will be noted that superimposed on each of the measured and faired signatures is an adjusted signature. A shock front is known to be extremely thin, and measured signatures would be expected to display a sharply defined pressure rise in the vicinity of a shock were it not for the effects of model and probe vibration and probe boundary layer which cause the pressure rise to spread over a finite distance. A method of reconstructing an idealized inviscid steady uniform flow signature from measured data devised in reference 27 has been applied to these data. The adjustment consists of extending forward the pressure curve behind the shock and inserting a vertical line to represent an adjusted shock so that the area under the original signature is preserved. For the $h/l = 2$ signature, the complete adjusted signature is not shown; however, the estimated peak value of $\Delta p_A/p$ is given. For this signature, uncertainties in forward extrapolation of the signature behind the shock preclude any accurate determination of the adjusted shock pressure rise. Adjusted signatures can be adequately defined for the remaining distances.

Before continuing with the discussion of results, it seems appropriate to discuss the selection of the measuring probe used in these tests, and the problems encountered in attempting to accurately measure static pressures in flow fields with strong shocks and large flow angularities. One of the problems in wind-tunnel sonic-boom measurement is to provide an adequate definition of the pressure rise across and the location of a relatively thin inclined shock front. Orifices in multiple orifice probes are commonly arranged in a plane inclined at the Mach angle or the shock angle to provide a better definition of the pressure rise across the shock. When measurements are to be made at more than one Mach number, more than one probe or, more practically, a compromise design is required. Even for this test at a single free-stream Mach number, the local shock front angle varied from about 33° to 14°. Earlier unreported studies have shown that a two orifice probe which does not have this problem (a line connecting the two orifices is perpendicular to the plane containing the probe and the model, and thus both orifices remain in the shock front for any shock angle) provides static pressure measurements in moderate strength flow fields essentially identical to those provided by other probe designs including the commonly used four orifice probe with 90° circumferential spacing. The performance of the two orifice probe in strong shock fields had not been evaluated, but, because of the aforementioned advantage, was chosen for these tests.

Additional data gathered in these tests and presented in figure 3 serve to demonstrate the characteristics of the chosen probe and also to point out hazards associated with attempts to accurately measure static pressures in flow fields with strong shocks and the associated large flow angles. Here, pressure signatures measured with the two orifice probe ($\theta = 90^\circ$ and 270°) are compared with signatures obtained by a single orifice either facing the model ($\theta = 0^\circ$) or facing away ($\theta = 180^\circ$). The measured signatures are also compared with calculated signatures obtained by use of the finite-difference computing program

of reference 29. Even with the finest computational grid believed to be practical in view of computer time and cost, there is no assurance that a converged solution has been obtained. Finer grids result in decreasing peak overpressures and decreasing signature lengths. Nevertheless, the computed signature is believed to offer the best estimate that can presently be found for the close-in strong shock pressure signature ($h/l = 2$). Increasing reliance must be placed on the experimental data as the distance increases because of the numerical solution convergence problem and increasing reliability of the probe measurements.

For the two-body-length distance, where the finite-difference solution predicts flow angularity of 20.3° just behind the shock, it is seen that the $\theta = 0^\circ$ and the $\theta = 180^\circ$ measurements are vastly different. An overpressure ratio of about 13 is recorded by the orifice facing the model; whereas the orifice facing away records an overpressure ratio of less than 2. These differences are so large that the accuracy of any simple pressure-sensing probe is questionable. The two orifice probe registers pressures near the shock that appear to be too low by a factor of two or more. An arrangement of orifices (number, location, and size) could probably be devised to give reasonably accurate results over some Mach number and flow angularity range, but any universally applicable probe design for use in flow fields with strong shocks is unlikely. A better technique is to make the measurements at a location where the shock strength is weak enough to insure that the choice of probe design is not critical.

At the eight-body-length distance, the pressure variation with θ is much more subdued, the $\theta = 90^\circ$ and 270° data occupy a middle position, and the overpressure ratios have decreased to levels of one or less. The estimated flow angle of about 4.7° is not yet small, but is now comparable with the probe cone angle. Either the two orifice probe design or the conventional four orifice design would be expected to provide valid static-pressure measurements for overpressures and angularities of that magnitude and smaller.

The data presented and discussed indicate that sonic-boom measurements in a strong pressure field with large flow angularities should be avoided, even though the choice of smaller models (which provide larger nondimensionalized distances and thus weaker pressure fields) entails a sacrifice in the accuracy of the model construction and requires precision measurement techniques. Data presented in this report (see fig. 2(f)) and elsewhere (refs. 3 to 12) indicate that quite satisfactory measurements can be made with peak overpressure ratios no larger than 0.1. At that level, the measurement problems discussed herein are negligible. As a matter of interest, many of the references just cited show acceptable signature measurements with peak overpressure ratios considerably less than 0.01. At the higher end of the pressure spectrum, overpressure ratios of about one are perhaps marginal.

Overpressure and longitudinal distance scales used in the presentation of the basic data were chosen so that each of the signatures would be approximately the same size. This, however, camouflages the drastic changes that occur in both peak overpressure and signature length as h/l increases. To remedy this situation, a scaled pictorial representation of the model pressure field

development is given in figure 4. Note that peak overpressure expressed as a ratio to free-stream static pressure varies from a value of about 2 to a value of about 0.1 and that signature length varies from about 2 to 16 body lengths.

In spite of the drastic signature changes depicted in figure 4, it is possible (with the aid of the theory previously discussed) to define overpressure and longitudinal distance parameters which permit a reasonable superposition of all the signatures. Signatures plotted in this parametric form are shown in figure 5. Note the progressive nature of the signature development and the approach to the far-field theoretical form as h/l increases. Based on previous experience, it was somewhat surprising to find that even at 32 body lengths, the measured signature was still in a process of evolution to its ultimate theoretical form.

To further examine the evolution of the signatures with h/l and to permit some degree of extrapolation to larger h/l distances, the primary far-field signature parameters were plotted as a function of h/l in figure 6. In figure 6(a), it is seen that there is a gradual and continued growth in signature impulse parameter with h/l. But even at 32 body lengths the measured impulse is only about 65 percent of the far-field theoretical value. It appears that the impulse parameter will continue to increase with increasing h/l, but whether the full theoretical value will be reached is uncertain. As has been discussed, there is some question as to the accuracy of static-pressure measurements in the presence of strong shocks; thus, the impulse is also in question. However, these errors, if present, diminish rapidly with h/l, and thus the extrapolation should not be greatly affected.

The very low values of measured signature impulse shown in figure 6(a) for the smaller h/l values point out a previously unrecognized difficulty arising in attempts to use close-in measurements for large models in conjunction with present theoretical extrapolation methods (refs. 25, 30, and 31) to provide sonic-boom estimates. Because existing extrapolation methods are based on geometric acoustics, it was recognized that more accurate extrapolations would be made with smaller values of input overpressures provided they were accurately defined; thus, a compromise between large models for accurate overpressue definition and small models for weak disturbance generation (at larger relative distances) is required. For models generating lift, it was also recognized that the relative distance should be large enough to permit a reasonable approach to flow-field axial symmetry. The present extrapolation methods (with the exception of the relatively new and untested method of ref. 26) do not distinguish between volume- and lift-generated fields which behave very differently in the extreme near field. This requirement, in particular, brings about a strong bias in favor of the small model.

For very blunt bodies at high supersonic speeds, there is an additional factor complicating the model size selection problems. The additional factor is the variation with distance of the measured impulse. The impulse parameter $\int \frac{\Delta p}{p} \frac{dx}{l} \left(\frac{h}{l}\right)^{1/2}$ is one of the fundamental invariants in the extrapolation process. Thus, if the extrapolation input signature has an improper value of impulse, the whole extrapolation process is invalid. It is seen that the impulse

measured at $h/l = 2$ (again referring to fig. 6(a)) could be too small for extrapolation purposes by a factor of two or more even after accounting for possible inaccuracies of static-pressure measurements in the strong shock field. (The impulse parameter given by the not quite converged finite-difference solution is 3.5.) This consideration, which again argues for small models, is seen to place stringent demands on accurate construction of small models and on accurate measurement of very weak disturbances. There is, however, some hope that the extrapolation method of reference 26 which is based on the method of characteristics and allows for the presence of nonweak shocks, will provide a means of handling larger models and stronger pressure fields.

The best demonstration of a not quite expected but fortunate applicability of the simple far-field theory to the present situation is seen in figure 6(b). Here the bow-shock pressure rise of the adjusted experimental data plotted as a function of h/l is seen to asymptotically approach a value almost exactly equal to that given by the theory. Since the bow-shock pressure rise is commonly accepted as the single most important index of sonic-boom intensity, the implications of these data are very significiant. It appears that the earlier demonstrated applicability of far-field theory to prediction of sonic-boom intensity for slender bodies at moderate supersonic speeds may now be extended to bodies with ratios of diameter to length as great as two and to Mach numbers at least as high as 4.14. Although the correlation shown here has been obtained only for the uniform atmosphere of the wind tunnel, the conclusion is expected to apply also to the real atmosphere. References 2, 3, and 17, for example, show that far-field theoretical predictions for a uniform atmosphere are also applicable to the real atmosphere provided that account is taken of atmospheric propagation factors now given by the computer program of reference 25.

Variation with distance of the last of the far-field signature parameters, the signature length, is shown in figure 6(c). This parameter also appears to be approaching the far-field theory level, but is doing so very slowly.

Mention was made earlier of the contrast between the way far-field characteristics were approached for the body of the present experiment and the way they were approached for more slender bodies of previous tests. An example is shown in figure 7. For the present model and for a body of the same shape but with a diameter to length ratio of 0.16 (ref. 11), the impulse parameter is shown as a function of h/l. Inset sketches show the development of the signatures. Far-field theory impulse parameter levels and signatures are also shown. Signatures are shown in parametric form; thus, a single signature covers all distances for the theory. The character of the data for the present tests was discussed previously. Data for the more slender body are seen to be in marked constrast. The impulse parameter level is relatively constant and is quite close to the theoretical value. Extrapolation of signatures to large distances should create no trouble even for signatures taken as close as two body lengths. This figure clearly illustrates the extra care that must be taken in the planning of sonic-boom tests of blunt shapes to obtain meaningful data, whether that data is to be used for validation of theories or for extrapolation.

CONCLUSIONS

An experimental and theoretical study of sonic-boom generation of a blunt body at a high supersonic Mach number has provided the following conclusions:

1. For accurate measurement of sonic-boom flow fields with conventional static-pressure probes, strong pressure fields with large flow angularities should be avoided. Small models, for which larger nondimensionalized distances and thus weaker pressure fields can be obtained, are preferable to large models even with the sacrifice in construction accuracy and the demands placed on measurement systems. A discussion of model size compromises and some guidance on allowable overpressures are given in the text.

2. When the purpose of sonic-boom testing is the provision of data for use in existing geometric acoustic extrapolation methods, the limitations on overpressure are even more demanding because signature impulse is found to follow acoustical disturbance laws only for very weak flow fields.

3. The applicability of far-field sonic-boom theory previously demonstrated for more slender shapes may now be extended to bodies with ratios of diameter to length as great as two and to Mach numbers at least as high as 4.14.

The third conclusion is particularly significant in view of the implications of the first two which indicate serious limitations to the use of existing methods for the extrapolation of close-in experimental data.

Langley Research Center
National Aeronautics and Space Administration
Hampton, VA 23665
July 29, 1977

REFERENCES

1. Carlson, Harry W.: An Investigation of Some Aspects of the Sonic Boom by Means of Wind-Tunnel Measurements of Pressures About Several Bodies at a Mach Number of 2.01. NASA TN D-161, 1959.

2. Carlson, Harry W.: An Investigation of the Influence of Lift on Sonic-Boom Intensity by Means of Wind-Tunnel Measurements of the Pressure Fields of Several Wing-Body Combinations at a Mach Number of 2.01. NASA TN D-881, 1961.

3. Carlson, Harry W.: Wind-Tunnel Measurements of the Sonic-Boom Characteristics of a Supersonic Bomber Model and a Correlation With Flight-Test Ground Measurements. NASA TM X-700, 1962.

4. Morris, Odell A.: A Wind-Tunnel Investigation at a Mach Number of 2.01 of the Sonic-Boom Characteristics of Three Wing-Body Combinations Differing in Wing Longitudinal Location. NASA TN D-1384, 1962.

5. Carlson, Harry W.; and Morris, Odell A.: Wind-Tunnel Investigation of the Sonic-Boom Characteristics of a Large Supersonic Bomber Configuration. NASA TM X-898, 1963.

6. Carlson, Harry W.; and Shrout, Barrett L.: Wind-Tunnel Investigation of the Sonic-Boom Characteristics of Three Proposed Supersonic Transport Configurations. NASA TM X-889, 1963.

7. Carlson, Harry W.; Mack, Robert J.; and Morris, Odell A.: A Wind-Tunnel Investigation of the Effect of Body Shape on Sonic-Boom Pressure Distributions. NASA TN D-3106, 1965.

8. Morris, Odell A.: Wind-Tunnel Investigation of Sonic-Boom Characteristics of a Delta-Wing-Body Combination at Mach Numbers of 1.41 and 2.01. NASA TN D-3455, 1966.

9. Carlson, Harry W.; McLean, F. Edward; and Shrout, Barrett L.: A Wind-Tunnel Study of Sonic-Boom Characteristics for Basic and Modified Models of a Supersonic Transport Configuration. NASA TM X-1236, 1966.

10. Morris, Odell A.; Lamb, Milton; and Carlson, Harry W.: Sonic-Boom Characteristics in the Extreme Near Field of a Complex Airplane Model at Mach Numbers of 1.5, 1.8, and 2.5. NASA TN D-5755, 1970.

11. Shrout, Barrett L.; Mack, Robert J.; and Dollyhigh, Samuel M.: A Wind-Tunnel Investigation of Sonic-Boom Pressure Distributions of Bodies of Revolution at Mach 2.96, 3.83, and 4.63. NASA TN D-6195, 1971.

12. Miller, David S.; Morris, Odell A.; and Carlson, Harry W.: Wind-Tunnel Investigation of Sonic-Boom Characteristics of Two Simple Wing Models at Mach Numbers From 2.3 to 4.63. NASA TN D-6201, 1971.

13. Whitham, G. B.: The Flow Pattern of a Supersonic Projectile. Commun. Pure & Appl. Math., vol. V, no. 3, Aug. 1952, pp. 301-348.

14. Whitham, G. B.: On the Propagation of Weak Shock Waves. J. Fluid Mech., vol. 1, pt. 3, Sept. 1956, pp. 290-318.

15. Walkden, F.: The Shock Pattern of a Wing-Body Combination, Far From the Flight Path. Aeronaut. Quart., vol. IX, pt. 2, May 1958, pp. 164-194.

16. Hayes, Wallace D.: Linearized Supersonic Flow. Rep. No. AL-222, North Amer. Aviat., Inc., June 18, 1947.

17. Carlson, H. W.; and Maglieri, D. J.: Review of Sonic-Boom Generation Theory and Prediction Methods. J. Acoust. Soc. America, vol. 51, no. 2, pt. 3, Feb. 1972, pp. 675-685.

18. Hicks, Raymond M.; and Mendoza, Joel P.: Pressure Signatures for a .00053 Scale Model of the Saturn V-Apollo Launch Vehicle With Simulated Exhaust Plumes. NASA TM X-62,129, 1973.

19. Mendoza, Joel P.; and Hicks, Raymond M.: Wind-Tunnel Pressure Signatures for a 0.016-Scale Model of the Apollo Command Module. NASA TM X-62 047, July 14, 1971.

20. Hicks, Raymond M.; Mendoza, Joel P.; and Garcia, Frank, Jr.: A Wind-Tunnel Flight Correlation of Apollo 15 Sonic Boom. NASA TM X-62,111, 1972.

21. Garcia, Frank, Jr.; Hicks, Raymond M.; and Mendoza, Joel P.: A Wind Tunnel Flight Correlation of Apollo 16 Sonic Boom. NASA TM X-62,073, 1973.

22. Carlson, H. W.; and Morris, O. A.: Wind-Tunnel Sonic-Boom Testing Techniques. J. Aircr., vol. 4, no. 3, May-June 1967, pp. 245-249.

23. Morris, Odell A.; and Miller, David S.: Sonic-Boom Wind-Tunnel Testing Techniques at High Mach Numbers. J. Aircr., vol. 9, no. 9, Sept. 1972, pp. 664-667.

24. Middleton, Wilbur D.; and Carlson, Harry W.: A Numerical Method for Calculating Near-Field Sonic-Boom Pressure Signatures. NASA TN D-3082, 1965.

25. Hayes, Wallace D.; Haefeli, Rudolph C.; and Kulsrud, H. E.: Sonic Boom Propagation in a Stratified Atmosphere, With Computer Program. NASA CR-1299, 1969.

26. Ferri, A.; Ting, L.; and Lo, R. W.: Nonlinear Sonic Boom Analysis Including the Asymmetric Effects. AIAA Paper No. 76-587, July 1976.

27. Carlson, Harry W.: Correlation of Sonic-Boom Theory With Wind-Tunnel and Flight Measurements. NASA TR R-213, 1964.

28. Jones, L. B.: Lower Bounds for Sonic Bangs. J. Roy. Aeronaut. Soc., vol. 65, no. 606, June 1961, pp. 433-436.

29. Marconi, Frank; Salas, Manuel; and Yaeger, Larry: Development of a Computer Code for Calculating the Steady Super/Hypersonic Inviscid Flow Around Real Configurations.
Volume I - Computational Technique, NASA CR-2675, 1976.
Volume II - Code Description. NASA CR-2676, 1976.

30. Hicks, Raymond M.; and Mendoza, Joel P.: Prediction of Aircraft Sonic Boom Characteristics From Experimental Near Field Results. NASA TM X-1477, 1967.

31. Thomas, Charles L.: Extrapolation of Sonic Boom Pressure Signatures by the Waveform Parameter Method. NASA TN D-6832, 1972.

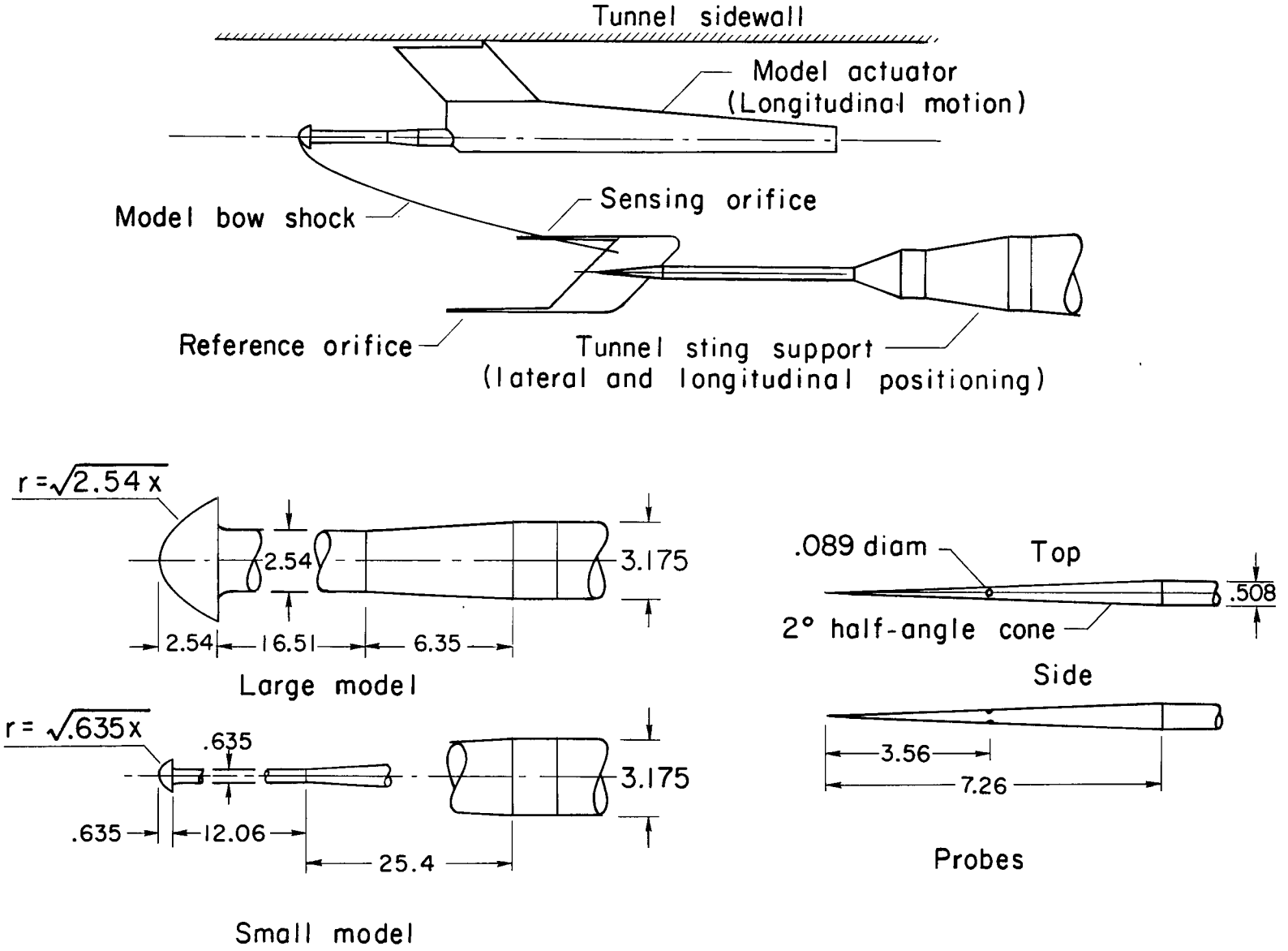

Figure 1.- Models and test apparatus. All dimensions are in cm.

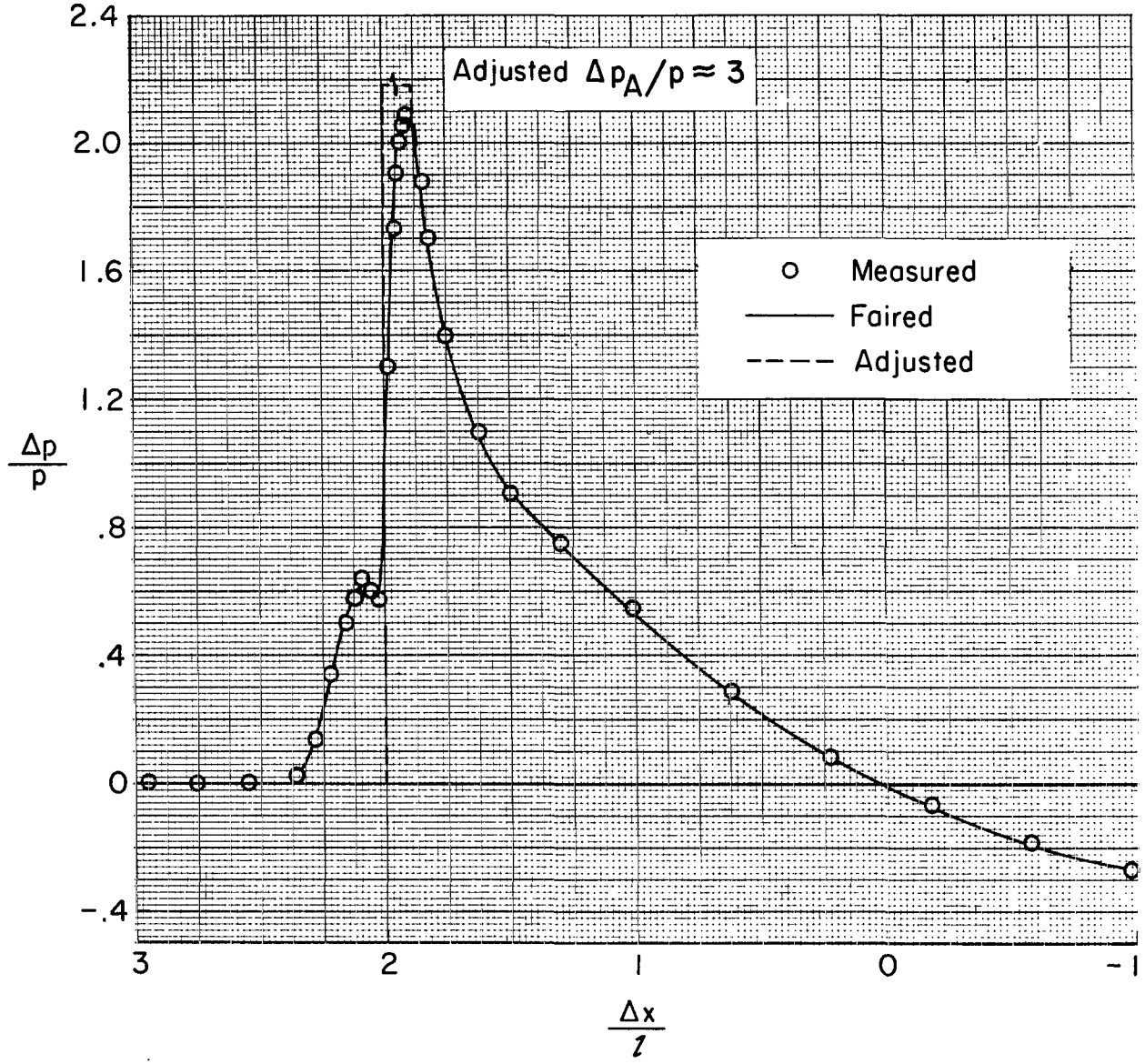

(a) Large model; h/l = 2.

Figure 2.- Measured signatures at various distances.

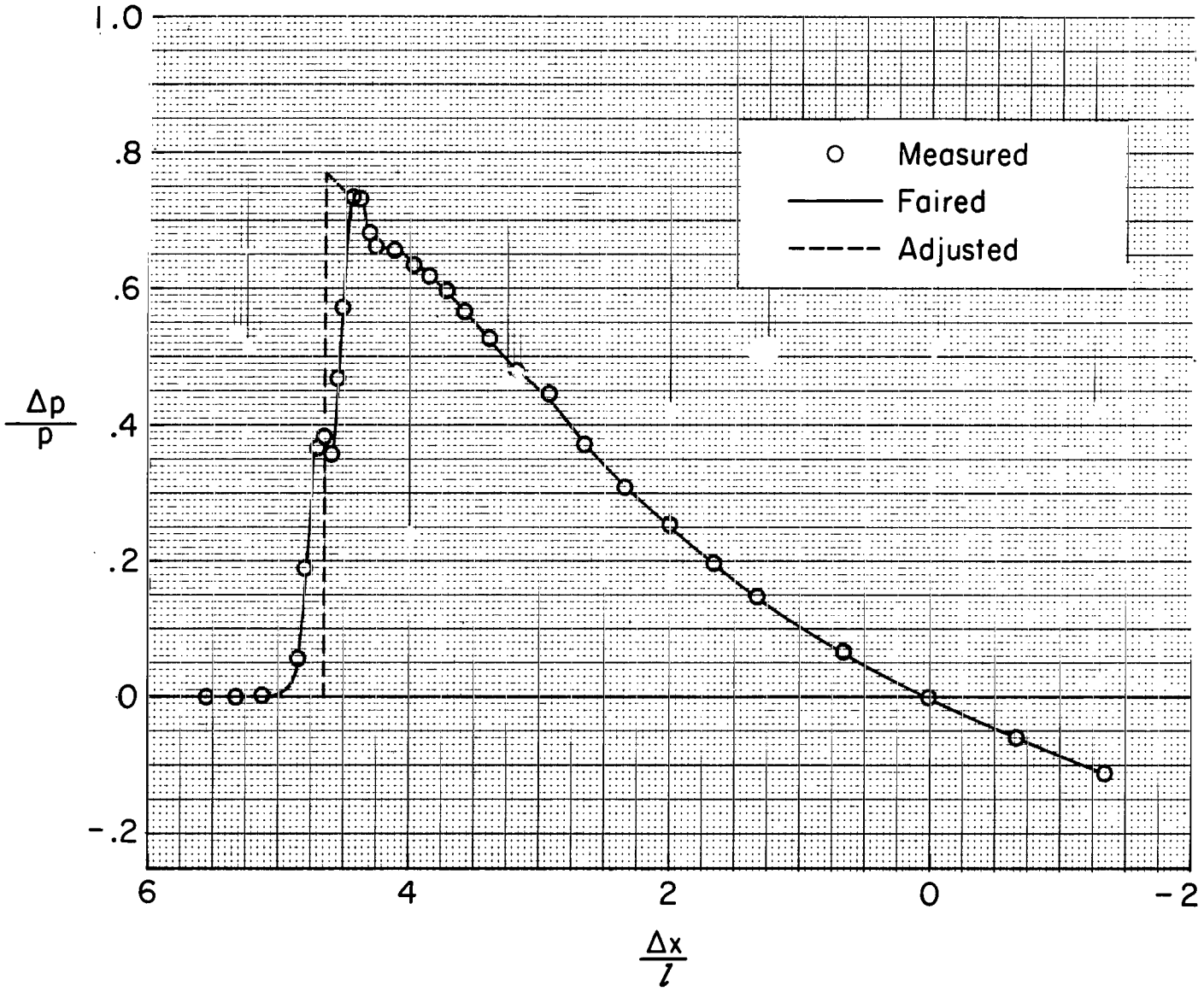

(b) Large model; $h/l = 4$.

Figure 2.- Continued.

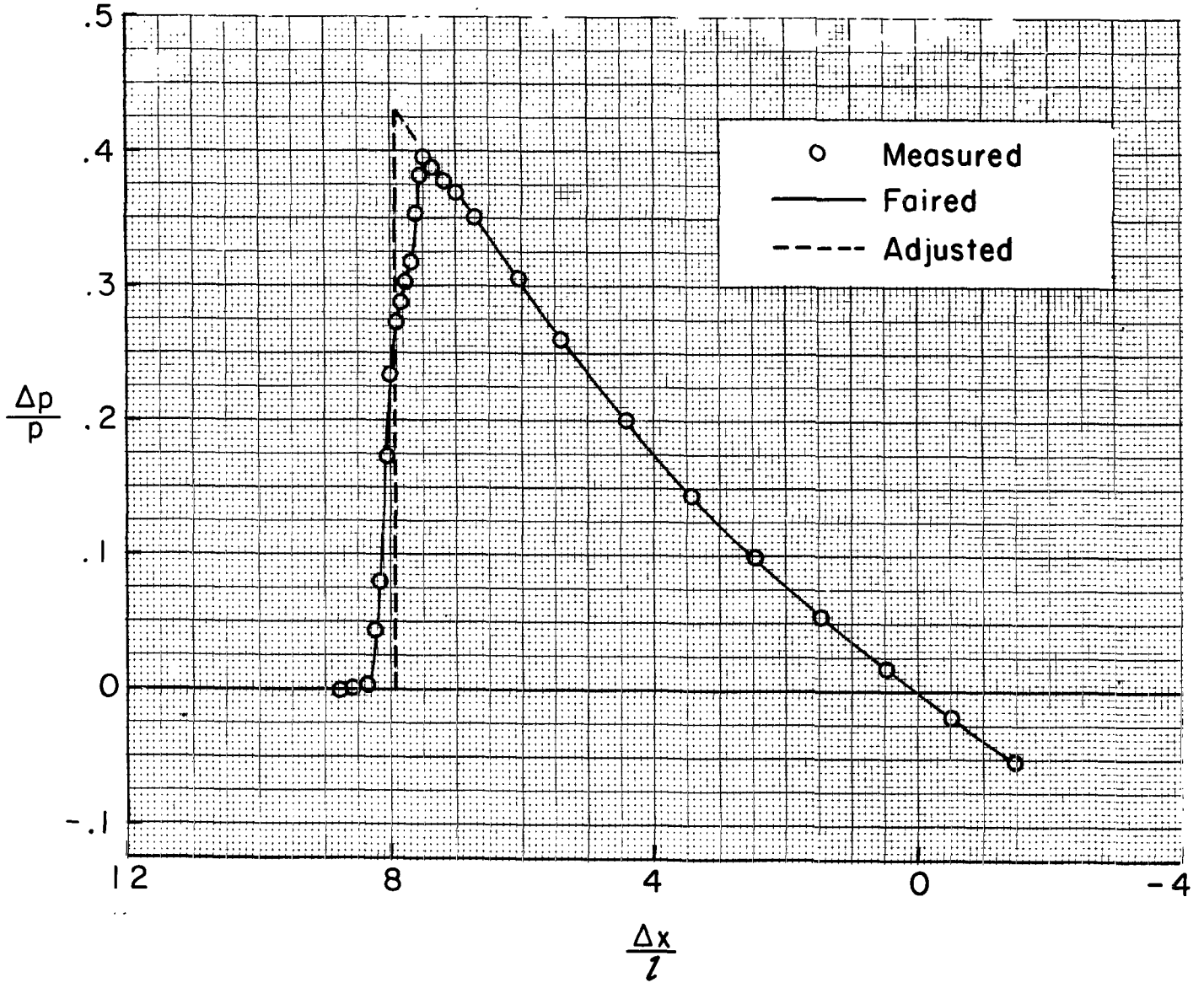

(c) Large model; $h/l = 8$.

Figure 2.- Continued.

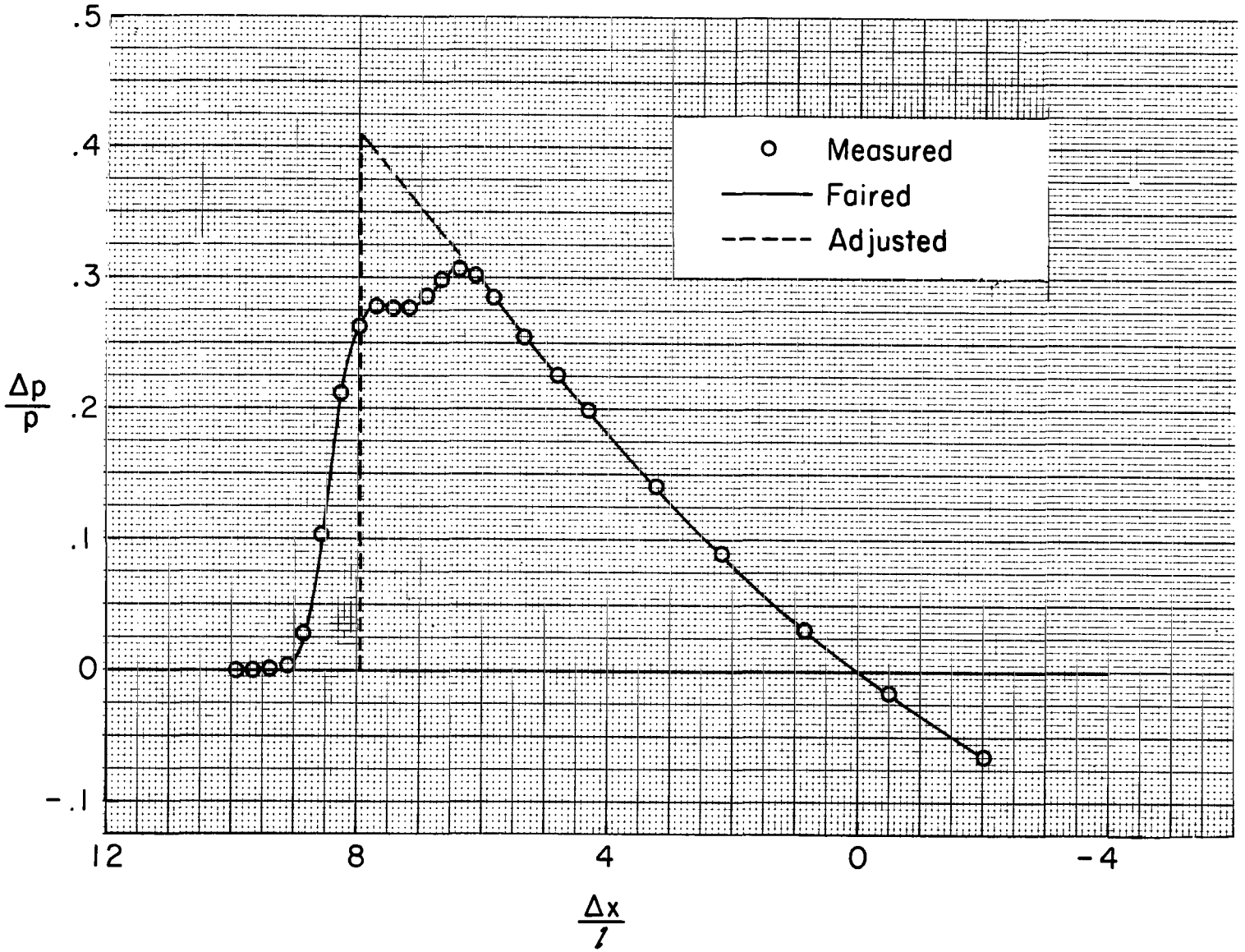

(d) Small model; $h/l = 8$.

Figure 2.- Continued.

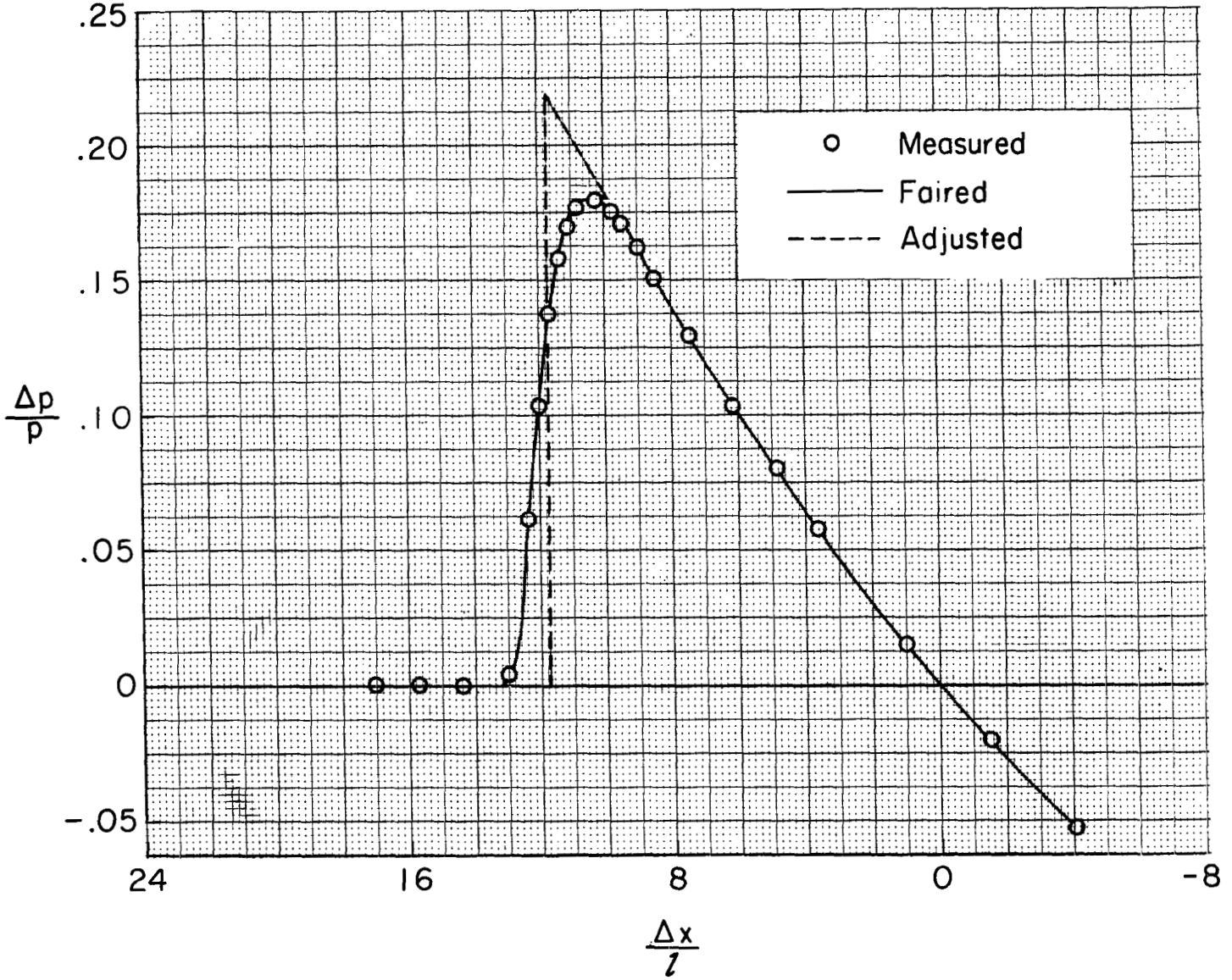

(e) Small model; $h/l = 16$.

Figure 2.- Continued.

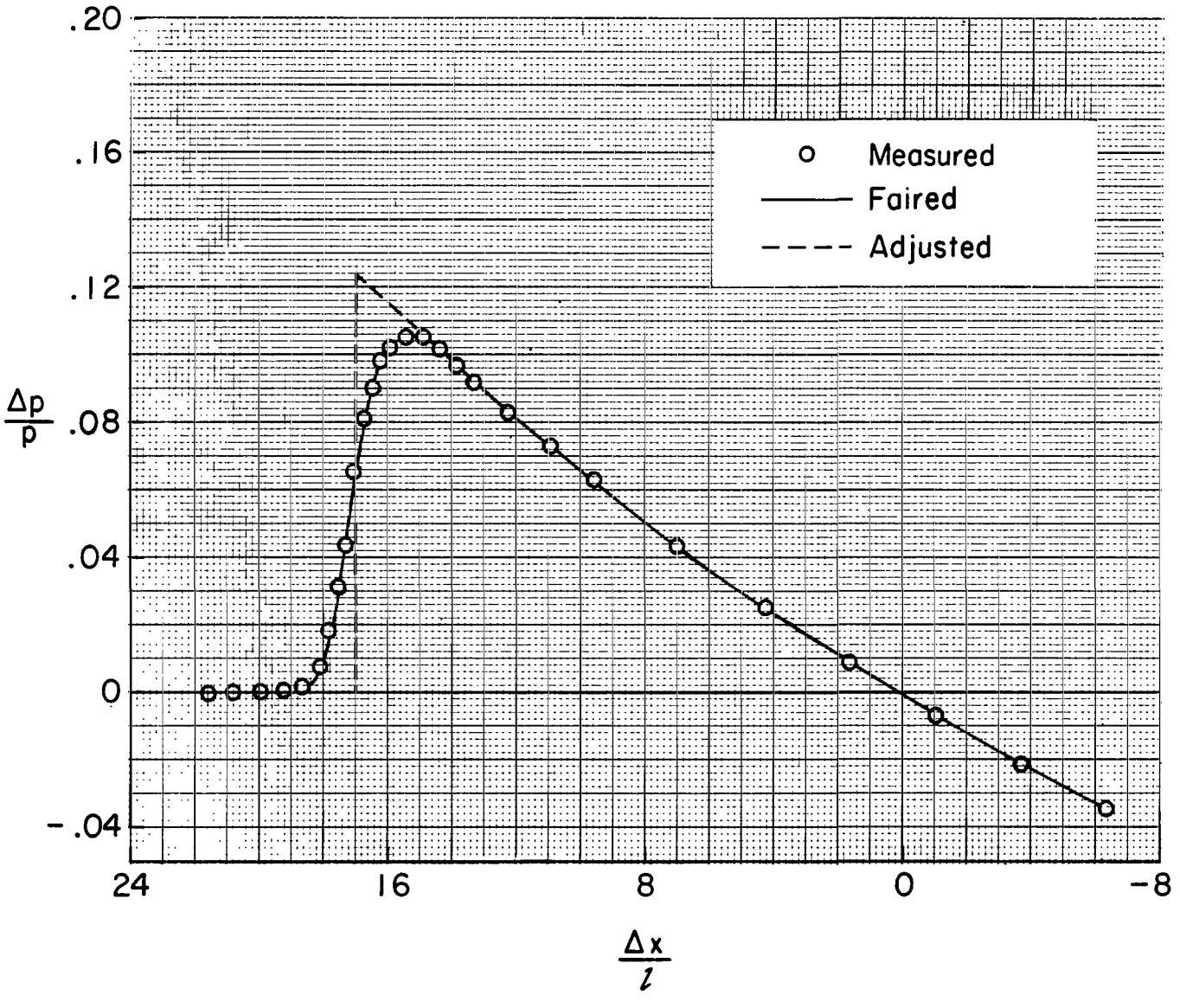

(f) Small model; $h/l = 32$.

Figure 2.- Concluded.

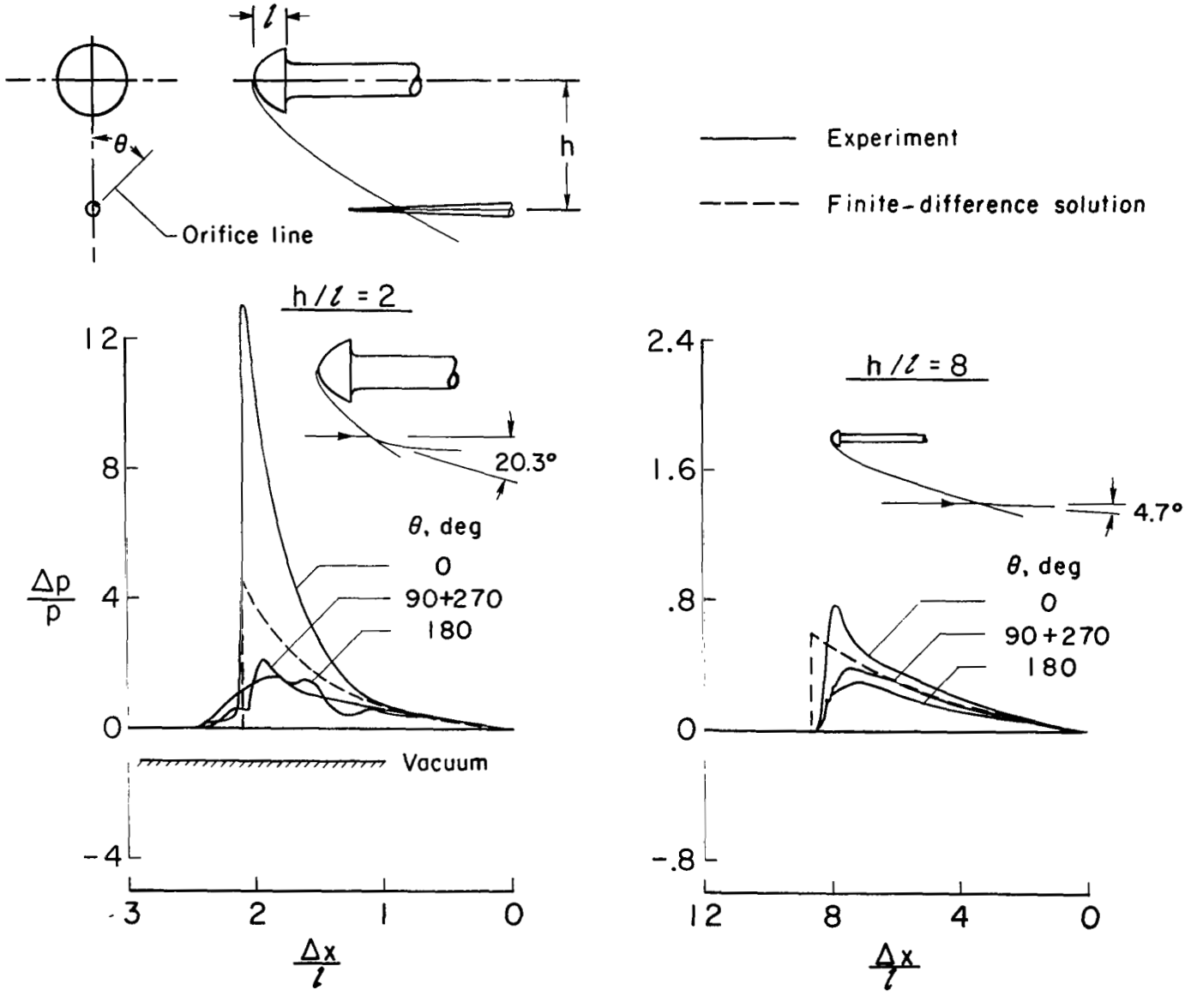

Figure 3.- Sensitivity of near-field pressure measurements to orifice location and probe design.

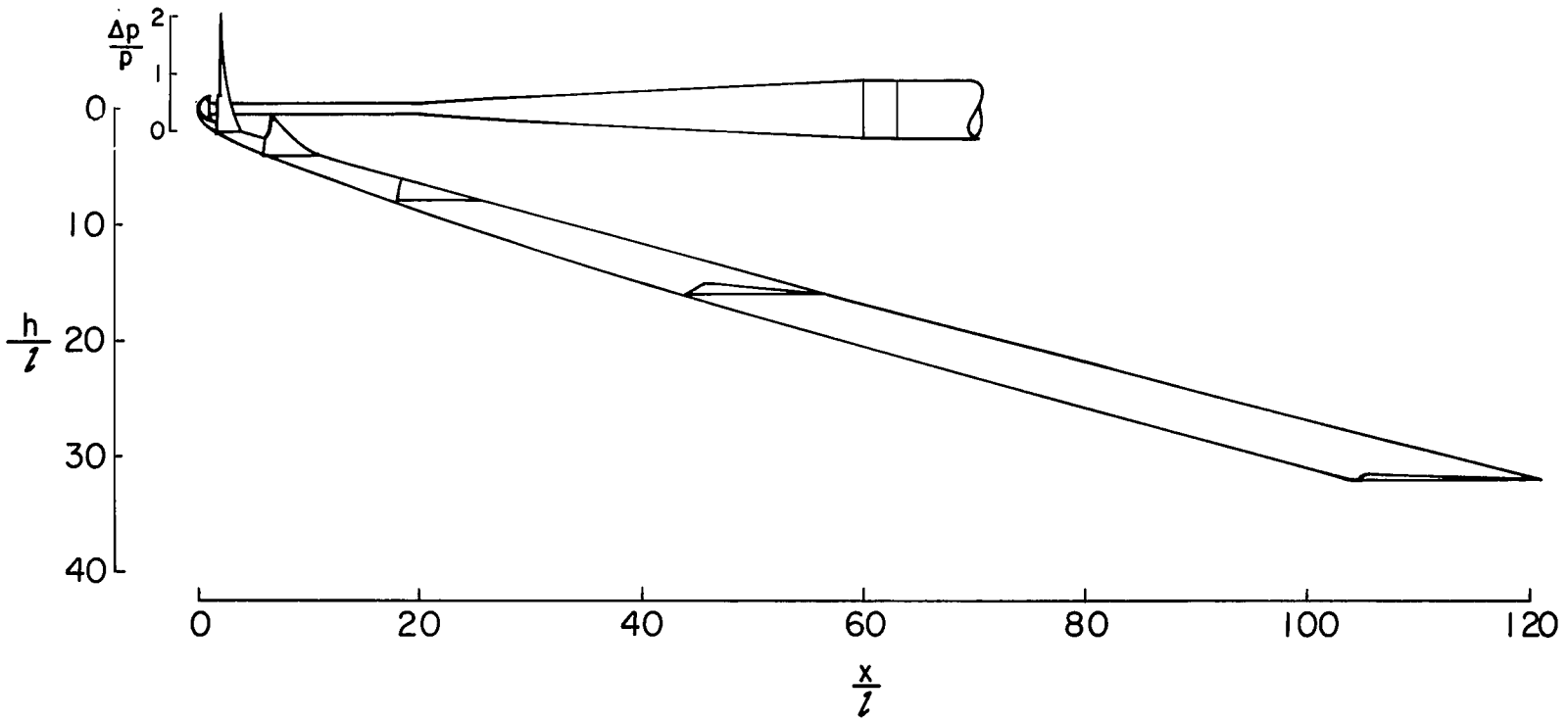

Figure 4.- Scaled pictorial representation of model pressure field.

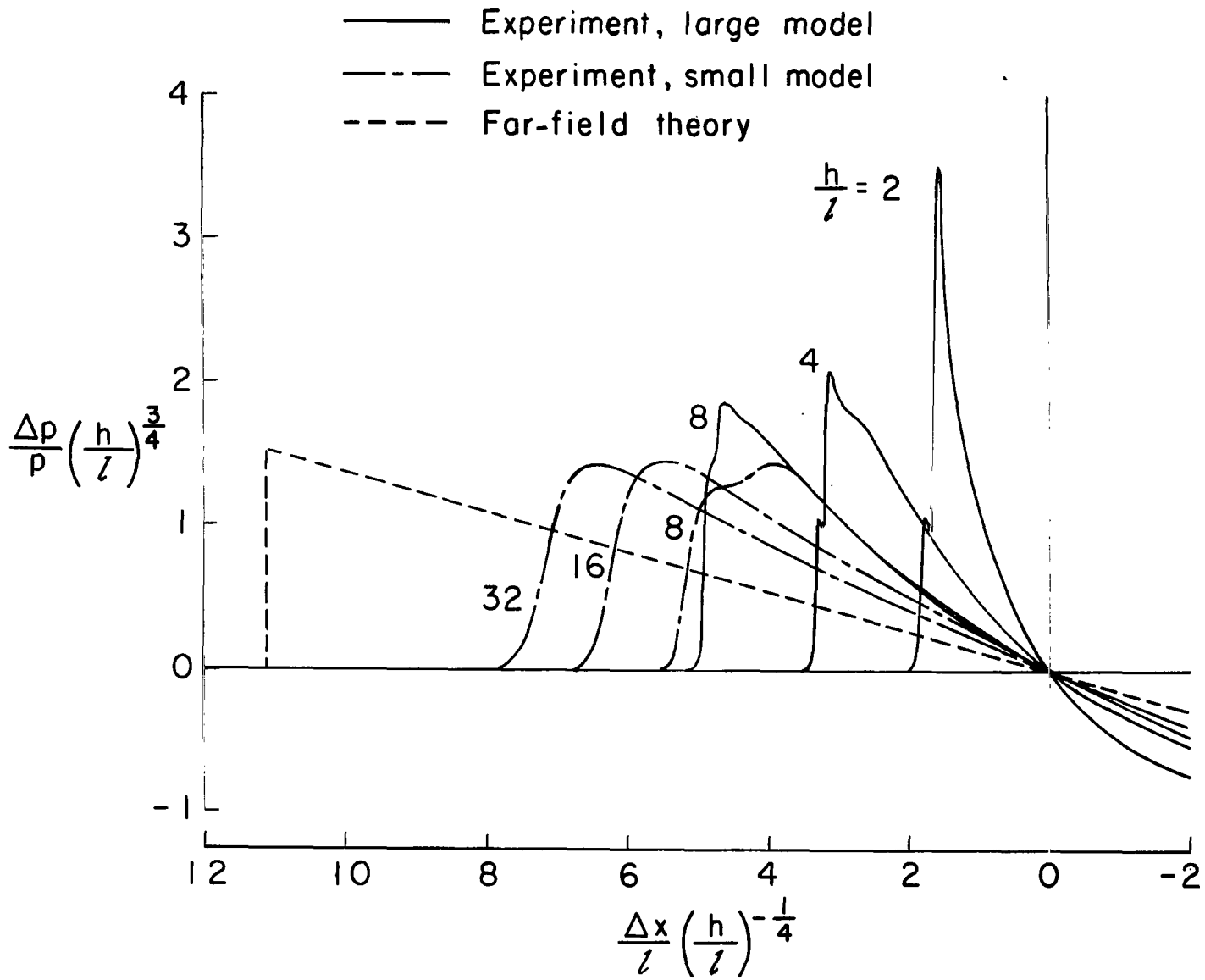

Figure 5.- Signatures in far-field parametric form.

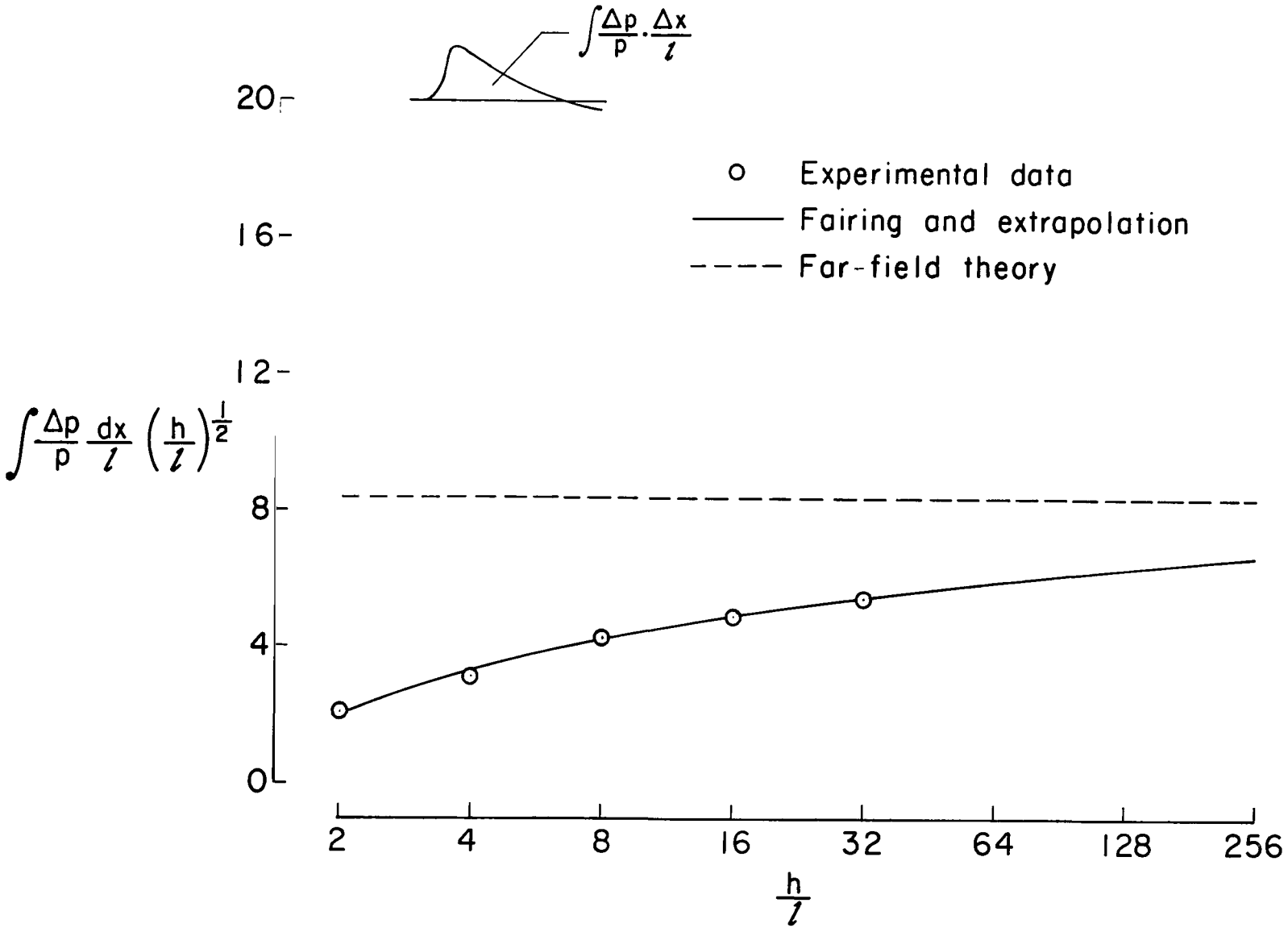

(a) Impulse.

Figure 6.- Variation of far-field signature parameters with distance.

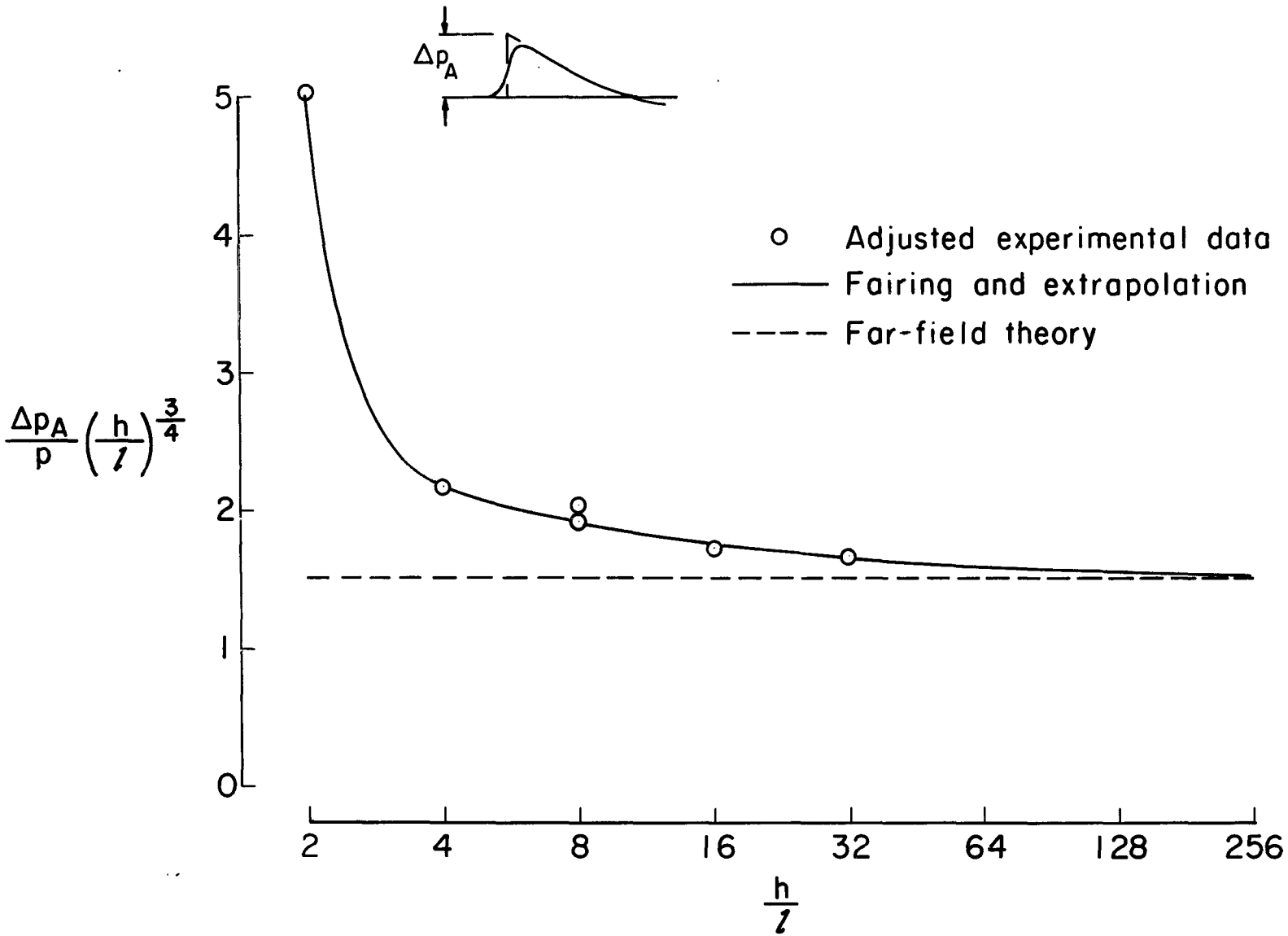

(b) Overpressure.

Figure 6.- Continued.

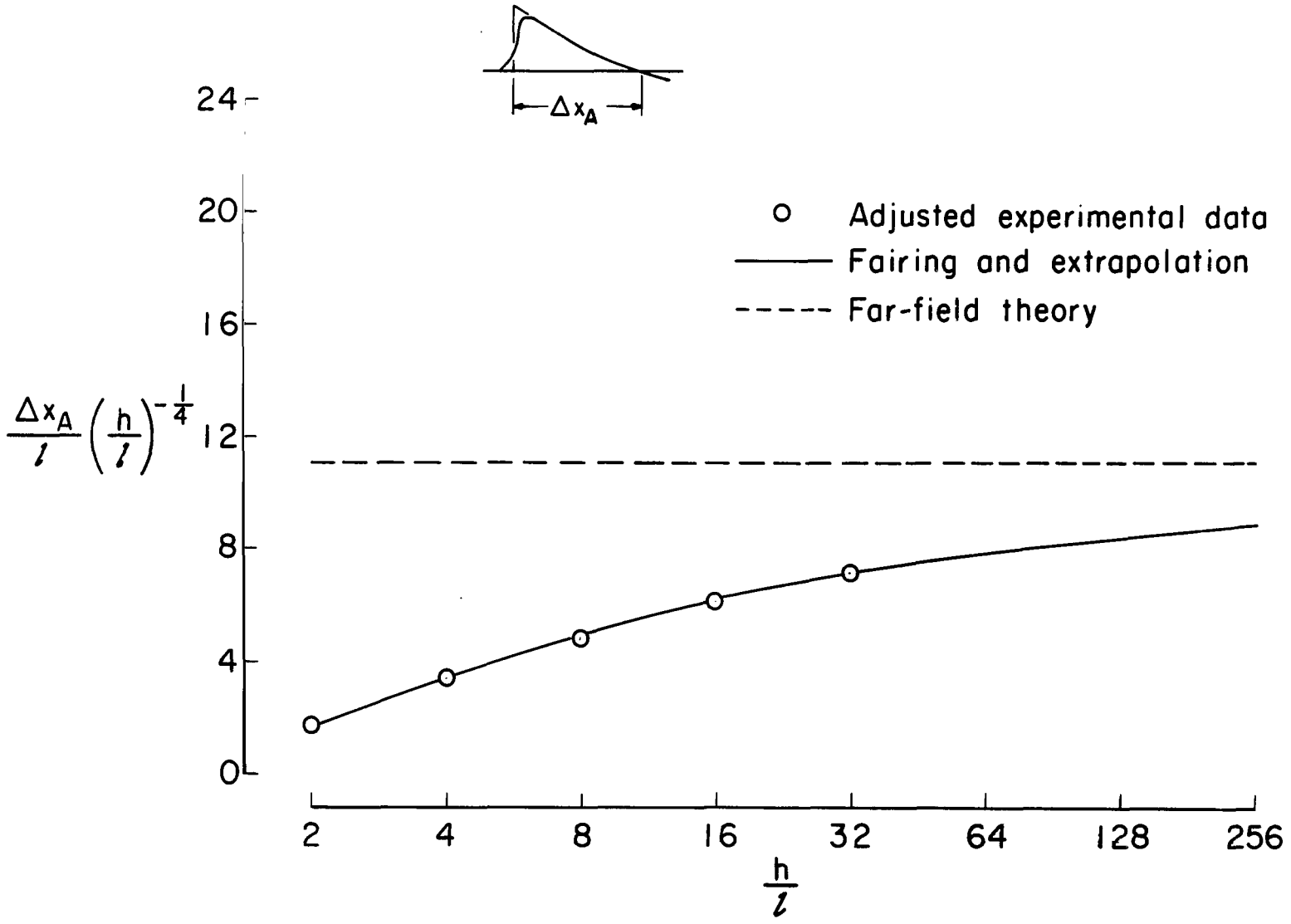

(c) Length.

Figure 6.- Concluded.

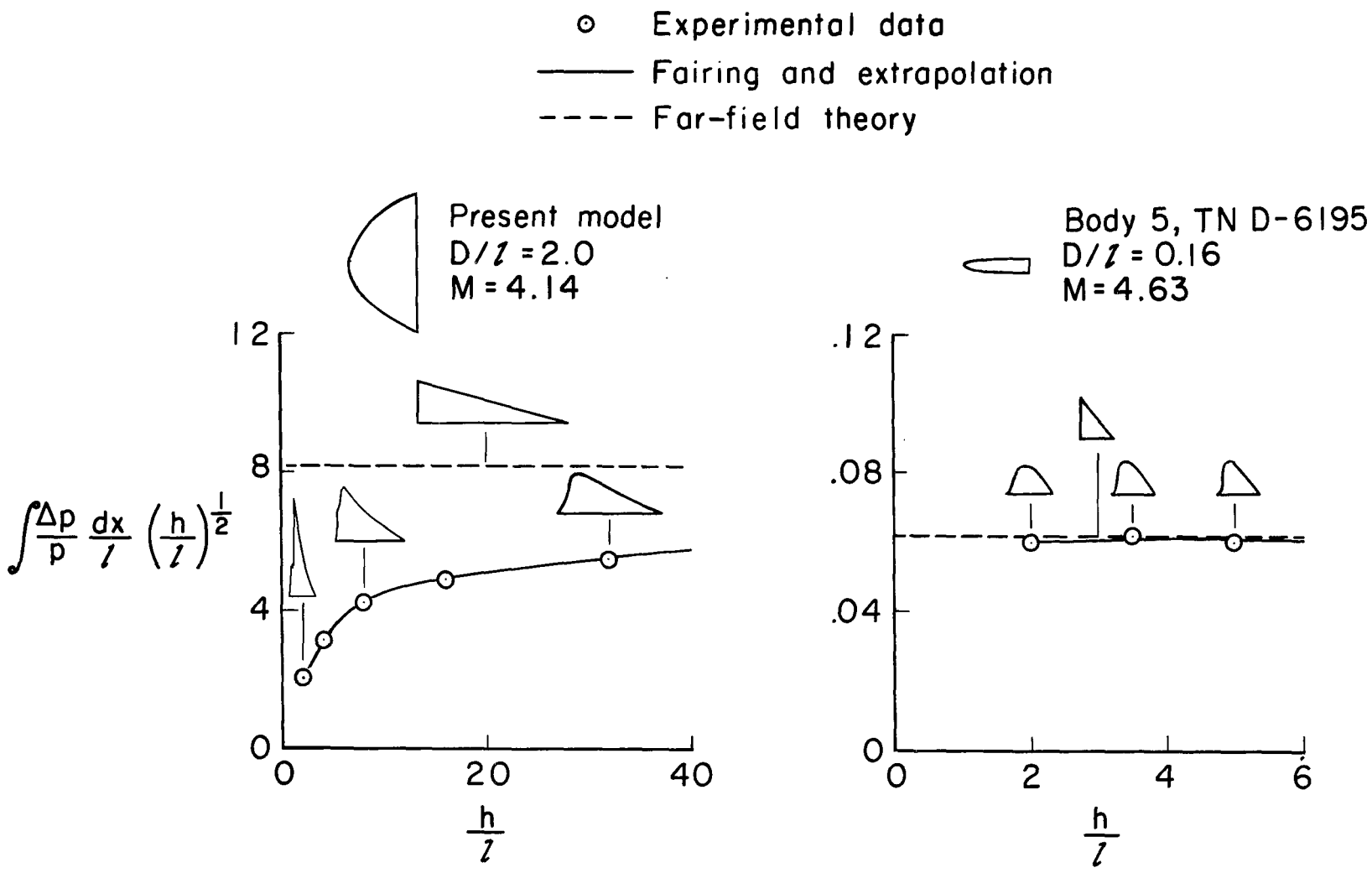

Figure 7.- Approach to far-field conditions for the present model contrasted to that for a slender body.

1. Report No.	2. Government Accession No.	3. Recipient's Catalog No.
NASA TP-1015		

4. Title and Subtitle	5. Report Date
A STUDY OF THE SONIC-BOOM CHARACTERISTICS OF A BLUNT BODY AT A MACH NUMBER OF 4.14	September 1977
	6. Performing Organization Code
7. Author(s)	8. Performing Organization Report No.
Harry W. Carlson and Robert J. Mack	L-11456
	10. Work Unit No. 743-04-31-01
9. Performing Organization Name and Address	11. Contract or Grant No.
NASA Langley Research Center Hampton, VA 23665	
	13. Type of Report and Period Covered
12. Sponsoring Agency Name and Address	Technical Paper
National Aeronautics and Space Administration Washington, DC 20546	14. Sponsoring Agency Code

15. Supplementary Notes

16. Abstract

An experimental and theoretical study of the sonic boom generated by a blunt body at a high supersonic Mach number has shown that the applicability of far-field sonic-boom theory previously demonstrated for more slender shapes may now be extended to bodies with ratios of diameter to length as great as two and to Mach numbers at least as high as 4.14. This finding is of special significance in view of the limitations to the use of existing methods for the extrapolation of close-in experimental data that were uncovered in the study.

17. Key Words (Suggested by Author(s))	18. Distribution Statement
Sonic boom Blunt bodies Pressure fields	Unclassified - Unlimited Subject Category 01

19. Security Classif. (of this report)	20. Security Classif. (of this page)	21. No. of Pages	22. Price*
Unclassified	Unclassified	28	$4.00

* For sale by the National Technical Information Service, Springfield, Virginia 22161

NASA-Langley, 1977

3 1 1U,A, 082677 S00903DS
DEPT OF THE AIR FORCE
AF WEAPONS LABORATORY
ATTN: TECHNICAL LIBRARY (SUL)
KIRTLAND AFB NM 87117